The Sodium Iodide Symporter (NIS) as an Imaging Reporter for Gene, Viral, and Cell-based Therapies

Alan R. Penheiter[1], Stephen J. Russell[1,2] and Stephanie K. Carlson[1,3,*]

[1]*Department of Molecular Medicine;* [2]*Division of Hematology;* [3]*Department of Radiology, Mayo Clinic, Rochester, MN 55905*

Abstract: Preclinical and clinical tomographic imaging systems increasingly are being utilized for non-invasive imaging of reporter gene products to reveal the distribution of molecular therapeutics within living subjects. Reporter gene and probe combinations can be employed to monitor vectors for gene, viral, and cell-based therapies. There are several reporter systems available; however, those employing radionuclides for positron emission tomography (PET) or single-photon emission computed tomography (SPECT) offer the highest sensitivity and the greatest promise for deep tissue imaging in humans. Within the category of radionuclide reporters, the thyroidal sodium iodide symporter (NIS) has emerged as one of the most promising for preclinical and translational research. NIS has been incorporated into a remarkable variety of viral and non-viral vectors in which its functionality is conveniently determined by *in vitro* iodide uptake assays prior to live animal imaging. This review on the NIS reporter will focus on 1) differences between endogenous NIS and heterologously-expressed NIS, 2) qualitative or comparative use of NIS as an imaging reporter in preclinical and translational gene therapy, oncolytic viral therapy, and cell trafficking research, and 3) use of NIS as an absolute quantitative reporter.

Keywords: Gene therapy, imaging, NIS, oncolytic virus, PET, reporter gene, SPECT, sodium iodide symporter.

INTRODUCTION

Advances in preclinical and clinical tomographic imaging systems have enabled non-invasive imaging of reporter gene products to reveal the temporal and spatial biodistribution of molecular therapies in virtually any location within living subjects. Imaging of molecular therapies is critical to our understanding of patient-to-patient variability in treatment response, the development of new treatment strategies, and for patient safety monitoring. The three most common reporter gene imaging approaches use genes that encode an enzyme, receptor, or transport protein, and each of these approaches has its strengths and weaknesses [1, 2]. Ironically, one of the oldest examples of an imaging reporter gene in humans, the sodium iodide symporter (NIS), has emerged as one of the most exciting and promising reporter genes in preclinical and translational research. NIS is normally expressed on the basolateral surface of thyroid follicular cells and mediates uptake of plasma iodide (its physiologic substrate). In addition to iodide, NIS has the ability to transport several other atoms or molecules including perchlorate, perrhenate, astatide, tetrafluoroborate, and pertechnetate.

There have been many excellent review articles on NIS published over the past 10 years [3-23]. These articles describe in great detail the molecular structure, function, and regulation of NIS, particularly as it applies to imaging and therapy of the normal and diseased thyroid gland. This review will provide a basic overview of the structure and function of NIS, but will focus on 1) differences between endogenous NIS and heterologously-expressed NIS, 2) qualitative or comparative use of NIS as an imaging reporter to monitor temporal and spatial vector distribution in preclinical and translational gene therapy, oncolytic viral therapy, and cell trafficking research, and 3) the use of NIS as a sensitive and quantitative reporter to determine the number of vector-engaged cells in a given volume of tissue.

STRUCTURE, FUNCTION AND REGULATION OF NIS IN THE THYROID

The biosynthesis of thyroid hormones has been extensively described in medical textbooks and in the literature [5, 24, 25]. The following is a brief summary of the role of NIS in that process. NIS is an intrinsic plasma membrane glycoprotein containing 13 membrane spanning alpha helices and 3 N-linked glycosylation sites. NIS is normally located on the basolateral surface of thyroid follicular cells and co-transports two sodium ions down the electrochemical gradient and one iodide ion up the electrochemical gradient from the plasma into the cell. The process is referred to as iodide transport, and mutations in NIS are causative for congenital iodide transport defects [10, 23, 26]. The iodide transport process is driven by energy dependent transport of sodium ions through the activity of the Na^+/K^+-ATPase, which is also located on the basolateral membrane of the thyroid follicular cell. The main regulator of NIS expression in the thyroid is the thyroid stimulating hormone (TSH) [27, 28]. TSH stimulation of the TSH receptor initiates a G-protein-mediated signaling cascade that ultimately results in an increase in NIS mRNA and protein in thyroid follicular cells, and regulates the post-transcriptional phosphorylation and plasma membrane targeting of NIS [29-33].

*Address correspondence to this author at the Mayo Clinic, 200 First Street SW, Rochester, MN 55905; Tel: 507-284-8317; Fax: 507-266-4609; E-mail: scarlson@mayo.edu

1875-5631/12 $58.00+.00

TRAPPING AND STORAGE OF IODIDE AND IODINATED MOLECULES IN THE THYROID

After iodide is transported by NIS into the cytoplasm of the follicular cell, it is either oxidized or it flows down the electrochemical gradient to the thyroid lumen (or colloid) where, under normal physiological conditions, it is oxidized and stored in the form of iodinated tyrosyl residues on thyroglobulin for eventual catabolism into thyroid hormones. The two-component vectorial transport of inorganic iodide from blood to follicular cell cytoplasm to extracellular thyroid lumen is referred to as the thyroid trap [34-36] and serves as the foundation for the timing of the clinical pertechnetate scan, generally performed 20 min post IV injection of 1-5 mCi of $^{99m}Tc0_4$. Quantitative estimates indicate that under normal conditions approximately 90% of the thyroid $^{99m}Tc0_4$ signal at 20 min is in the extracellular compartment [34-36]. $^{99m}Tc0_4$ is a valuable imaging tool to measure this effect since it is efficiently transported by NIS but is not oxidized or incorporated into biological molecules and thus can resolve the rapid and reversible trapping activity of the thyroid from the long-term storage component. There have been many reports in the endocrinology and nuclear medicine literature describing molecular imaging techniques to distinguish iodide transport, trapping, and storage functions in the normal and pathologic thyroid tissue [37-43]. For a thorough summary, the interested reader is referred to the excellent prospective study by Reshchini *et al.* [44].

ENDOGENOUS NONTHYROIDAL NIS BIODISTRIBUTION AND FUNCTION

NIS is also normally expressed in the salivary glands, stomach, and lactating mammary glands at levels sufficient to visualize these organs with radioiodide if imaging is performed shortly (within a few hours) after administration of radioiodide [45]. NIS in the stomach and salivary glands is thought to function in an entero-thyroid recirculation loop to prolong the retention of iodide prior to renal elimination [46], while NIS in lactating mammary glands is thought to provide a source of dietary iodide in milk [45]. In addition, NIS has been documented, using immunohistochemistry and/or reverse-transcriptase polymerase chain reaction (RT-PCR), in several other human tissues including the lachrymal glands, choroid plexus, pituitary gland, ocular ciliary body, small intestine, pancreas, adrenal gland, heart, lung, thymus, prostate, ovary, kidney tubules, placenta, testis, and rectum. With the exception of the small intestine (absorption of iodide) and renal tubules (reabsorption of iodide) the physiological role, if any, of NIS in these additional tissues remains unknown [3, 47-53]. The primary differences between NIS expression and function in nonthyroidal tissues versus its role and function in the thyroid gland are that 1) nonthyroidal NIS is not regulated by TSH; rather it appears to be constitutively expressed in most of these other tissues, 2) nonthyroidal tissues have no or minimal ability to oxidize inorganic iodide to iodine, and 3) nonthyroidal tissues do not possess the specific machinery for storage of iodine in the form of iodinated compounds. However, like the thyroid gland, other tissues which endogenously express NIS (for example, stomach and salivary glands) do so in a highly polarized fashion, where the fate of NIS-transported iodide is secretion down the electrochemical gradient to an adjacent extracellular compartment (gastric juice, saliva) opposite the pole of NIS expression [54].

HETEROLOGOUS NIS IN TUMOR TISSUES

In contrast to the two-compartment trapping in the thyroid and the two-compartment secretion reaction in other tissues which endogenously express NIS, the majority of roles for NIS as an imaging *transgene* are for tumor cells which are not polarized. Thus, what is measured in a so-called iodide uptake assay of non-polarized cells *in vitro* and presumably what is seen on a SPECT image of a NIS-transduced xenograft is intracellular iodide. Interestingly, when directly comparing one-compartment intracellular iodide accumulation (*in vitro* assay), overexpression of NIS in a non-thyroidal cell line often results in an even higher magnitude of iodide uptake than that observed in thyroid cell lines [55]. This high level of transport activity combined with the high density of cells in many tumor types consistently provide a window of sensitivity for the detection of NIS-mediated accumulation of radioiodide or $^{99m}Tc0_4$, despite the lack of a second compartment. While the majority of reports on the NIS transgene have focused on tumor cells and tumor models, a number of recent reports have explored its use as a reporter gene or surrogate gene for gene therapy and cell trafficking protocols. These normal tissue applications of NIS add an additional level of complexity to the mechanistic study of heterologously-expressed NIS, where polarized cells and second compartments could play a role in NIS-mediated imaging.

THE BEGINNING OF NIS AS AN IMAGING REPORTER

The NIS gene was first cloned from the rat by Dai *et al.* in 1996 [56]. This was followed by cloning of human NIS later that year by Jhiang, *et al.* [57] and the cloning of mouse NIS by Pinke, *et al.* in 2001 [58]. Transient and stable NIS expression in nonthyroidal tissues and tumor xenografts stimulates significant iodide uptake *in vivo*, although to a lesser degree than *in vitro* NIS-mediated uptake, and has led to the use of NIS as an imaging reporter in numerous preclinical and two clinical research protocols [7, 55, 59-106].

Shimura, *et al.* [59] were the first to demonstrate *in vivo*, non-invasive molecular imaging with the NIS transgene. While working with FRTL cells (an untransformed, TSH dependent, "normal" thyroid epithelial cell line originating in Fisher 344 rats) [107], they noted the appearance of a cell type with altered morphology, a loss of thyroglobulin expression, and a reduction in the requirement of exogenous TSH beginning at passage 50. These altered cells were grown for an additional 40 passages in the absence of TSH giving rise to a population of cells (denoted FRTL-Tc) that did not require TSH, likely due to compensatory adrenergic responsiveness and elevated baseline cAMP. The cells; however, still responded to TSH. Also, they were no longer subject to contact inhibition, and were capable of growing as syngeneic and metastatic tumors in Fischer 344 rats. This was the first report of a malignant thyroid cell line with documented retention of the TSH receptor. Further charac-

terization of the cell line revealed that, in addition to loss of thyroglobulin, the cells had lost the ability to accumulate iodide in an *in vitro* uptake assay [59]. This prompted the investigators to stably transfect the FRTL-Tc line with the recently cloned rat NIS gene, which restored *in vitro* iodide transport activity to a level greater than that observed in the TSH-stimulated parental FRTL cells. Tumors were then grown from these cells in Fischer 344 rats. The rats were given a tracer dose of ^{125}I, and serum and tumor ^{125}I concentrations were determined. A group of animals was anesthetized and serially imaged on a phosphorimaging cassette. This allowed the investigators to monitor the time course of the appearance and disappearance of radioactivity in the tumor, thyroid, and whole body. Additional rats were euthanized and absolute radioactivity levels were determined *ex vivo*. At peak tracer uptake (2 h post-injection of ^{125}I) the FRTL-Tc-NIS tumors exhibited a mean of 19.3-times the serum ^{125}I concentration and a remarkable 48.3-times the control FRTL tumor concentration. Thus, if one assumes a uniform concentration of radiotracer and that each tumor cell is an independent iodide transporting entity, then one can calculate in this model that as few as 5% NIS-expressing cells will result in a tumor that appears twice as "hot" as serum. Likewise, using the same 2-fold above background as a threshold, only 2% NIS-transduced cells would be required to resolve a NIS tumor from a control tumor. These landmark studies firmly established NIS as a sensitive and quantitative imaging reporter. Mandell (1999) [60] went on to document the *in vivo* visualization of stable NIS-transduced melanoma xenografts using ^{123}I scintigraphy with a clinical gamma camera. The following year, Boland *et al.* (2000) and Spitzweg *et al.* (2000) [4, 55] published imaging results with non-replicating adenoviruses encoding NIS in cervical cancer, breast cancer, and prostate cancer xenografts. This was followed by the engineering of the first replication-competent oncolytic adenovirus expressing NIS and imaging of cervical cancer xenografts and dog prostate [66]. Soon after, the first engineered replicating oncolytic RNA virus (Edmonston-strain measles virus) expressing NIS (MV-NIS) was rescued by Dingli *et al.* (2004), [108] and images of MV-NIS infected myeloma xenografts were presented. These pioneering studies paved the way for an explosion in the use of NIS as a non-invasive imaging reporter over the next decade.

THE ROLE OF NIS AS AN IMAGING REPORTER GENE

The three main areas of preclinical and translational research to which NIS reporter imaging has been applied are viral-mediated gene therapy, oncolytic viral therapy, and cell trafficking (eg, stem cell delivery). Each of these will be discussed in further detail. The success of these research strategies depends on adequate delivery of the vector or transduced/ transfected cell to the target tissue, as well as persistent gene expression or viral infection in the target tissue. Noninvasive monitoring of gene expression or viral propagation over time in living animals is critical to facilitate the advancement of these new molecular therapies in human subjects.

NIS Reporter Imaging in Viral-Mediated Gene Therapy Research

The NIS reporter has been used for monitoring viral-mediated cancer gene therapy (defined here as the use of viral vectors that are not intended to lyse cells directly, but rather require expression of a therapeutic gene). In the vast majority of reports in this arena, NIS itself has been employed as the therapeutic gene with the intention of using therapeutic radioisotope concentration as the means of tumor ablation. Many of the pioneering studies in this field were instrumental in optimizing small-animal imaging methodologies that were later applied to all avenues of NIS research [4, 6, 55, 59, 64]. However, in these studies the unique reason for imaging was not to report but to "predict" the dose of a subsequently administered therapeutic isotope. As dosimetry is a fundamentally different concept than reporting (dosimetry requires the area under an imaging curve, and non-reporter background probe activity is included in the quantitative analysis) it is not the subject of this review. Interested readers, however, are referred to several recent reviews on the subject [16, 17, 109].

NIS also has been incorporated as an imaging reporter for conventional gene therapy protocols. In this context NIS can be used as a direct reporter for a gene delivery vector or to report on a second therapeutic gene. Niu *et al.* (2004) [75] investigated the use of NIS as a reporter to noninvasively image *in vivo* gene transfer and expression in lung tissue for the purposes of developing a gene therapy strategy for cystic fibrosis by potentially correcting a mutated CFTR gene and restoring its function [75]. These investigators used $^{99m}TcO_4$ scintigraphy and ^{124}I PET imaging to determine the location, magnitude, and duration of pulmonary gene transfer following the delivery of Ad-hNIS to the lungs of cotton rats. Lungs infected with Ad-hNIS were still visualized at 17 days post-instillation of the virus through the rat nostrils.

Another recent use of NIS reporter gene imaging has been in cardiovascular gene therapy research [83, 110-112]. Miyagawa *et al.* (2005) [110] first demonstrated the feasibility of NIS for myocardial gene expression imaging in rats using $^{99m}Tc0_4$ and ^{123}I scintigraphy and demonstrated a significant correlation between quantitative image analysis and *ex vivo* gamma counting of radioactivity in the NIS transfected hearts. Lee *et al.* (2005) [83] investigated the accuracy of scintigraphy for assessing myocardial gene expression in living rats using a dual-gene adenovirus that expressed both NIS and eGFP [83]. Results showed increased radioactivity uptake in a viral titer-dependent manner, and *ex vivo* analyses revealed a quantitative relationship between NIS mediated imaging and GFP expression. Rao *et al.* (2007) and Ricci *et al.* (2008) [111, 112] then went on to demonstrate the feasibility of micro-SPECT/CT imaging and quantitation of cardiac gene expression after NIS gene transfer in cardiac transplants in rats [111, 112]. Ricci *et al.* also demonstrated the high concordance between NIS reporter gene expression in the transplanted heart (measured on ^{123}I scintigraphy) and soluble reporter peptide levels in serum using a bicistronic adenoviral vector expressing NIS and either human carcinoembryonic antigen or beta human chorionic gonadotropin.

NIS Reporter Imaging in Oncolytic Viral Therapy Research

Because of their ability to selectively replicate and spread in cancer cells and their ability to amplify vector-associated transgene expression, replication-competent oncolytic viruses are being used increasingly in cancer therapy [113-118]. The ability to monitor the delivery and intratumoral propagation of oncolytic viruses is critical to understand the kinetics of oncolytic viral spread, determine the optimal viral dose for safety and maximal therapeutic effect, determine the timing of additional therapeutic strategies to enhance the oncolytic viral effect, and to improve future oncolytic viral design (targeted viruses, etc.). To achieve these goals, oncolytic viruses have been modified to express NIS.

Barton *et al.* (2003) were [66] the first to use NIS as a preclinical reporter to monitor and optimize oncolytic virus therapy. These investigators used a replication-competent adenovirus encoding a yeast cytosine deaminase (yCD)--herpes simplex virus thymidine kinase (*mut*TK_{SR39}) fusion protein and a second transgene encoding NIS in mouse xenograft and dog prostate models. This same group of investigators went on to publish two additional studies to further develop and optimize this adenovirus-mediated therapy protocol in small and large animal models [94, 119] and ultimately to demonstrate the safety and feasibility of NIS and $^{99m}TcO_4$ SPECT/CT as an imaging reporter system in humans [120, 121].

Dingli *et al.* (2004) [69] first rescued the recombinant Edmonston vaccine strain of measles virus (MV-Edm) encoding the NIS gene and demonstrated 1) the ability of MV-NIS to replicate almost as efficiently as unmodified MV-Edm, 2) human multiple myeloma tumor cells infected with MV-NIS efficiently localized radioiodide *in vitro*, and 3) MV-NIS expressing human myeloma xenografts in immunocompromised mice could be visualized *in vivo* using serial ^{123}I scintigraphic imaging. Dingli *et al.* demonstrated the ability of ^{124}I PET/CT to accurately image stably NIS-transfected and IV MV-NIS infected multiple myeloma xenografts [81]. Since these early experiments, other investigators have shown similar results supporting the use of MV-NIS as an imaging reporter in oncolytic viral therapy studies of ovarian cancer, pancreatic cancer, prostate cancer, and mesothelioma [88, 103, 122-124]. NIS also has been included as a reporter in other oncolytic viruses including vesicular stomatitis virus (VSVDelta51-NIS) [91], a variety of oncolytic adenoviruses [66, 92, 106, 125-127], and recently, oncolytic vaccinia virus [128].

NIS Reporter Imaging in Cell Trafficking Research

A further application of the NIS transgene reporter system that we will discuss is its use for monitoring the delivery and fate of transduced or transfected cells with therapeutic capabilities (eg, stem cells, immune cells). Stem cell transplantation is a promising therapeutic option for patients with impaired organ function (*eg*, heart, spinal cord) due to cell death; and the use of stem cell therapy in preclinical and clinical research is expanding [16, 129-131]. Stem cells are pluripotent or omnipotent cells obtained from bone marrow and peripheral blood (among other sites in the body) that can self-renew and differentiate into specialized cells (including tissue-regenerating cells) depending on their microenvironment. Similar to the questions that arise in gene and viral therapy research, being able to determine the 1) stem cell biodistribution and homing, 2) number of stem cells that were successfully engrafted and underwent differentiation, and 3) stem cell survival time are critical to the further advancement of this research field. Thus, reporter genes are needed to help track the fate of stem cells *in vivo* and maximize the functional benefit of stem cell therapy in patients.

Thus far, cell trafficking studies have used *in vitro* cell labeling with either iron oxide nanoparticles (for use with MRI imaging) or radionuclides (for use with nuclear medicine imaging modalities) [16, 129-131]. The problem with this approach is that it is nonspecific; the imaging signal can persist even after death of the labeled cell, impairing the ability to accurately quantitate successful stem cell engraftment. The imaging reporter gene approach can overcome this limitation because the transduced cell will only provide an image signal in viable reporter gene-expressing cells.

Stem cell therapy is a particularly hot topic in cardiovascular research because of its ability to improve cardiac function after myocardial infarction [129, 131]. Terrovitis *et al.* (2008) [129] was the first to report the use of NIS to track stem cells delivered to the rat heart with SPECT and PET imaging. The investigators transduced rat cardiac-derived stem cells (rCDCs) using lentiviral vectors and injected them intramyocardially (up to 4 million NIS+ rCDCs) immediately after left anterior descending coronary artery ligation. Cell viability and proliferation was not affected by NIS expression, and $^{99m}TcO_4$ SPECT and ^{124}I PET imaging demonstrated NIS-mediated uptake of radiotracer in the areas of myocardial perfusion deficit. Higuchi *et al.* (2009) [131] used NIS-mediated ^{124}I PET imaging to successfully monitor the delivery and survival of endothelial progenitor cells (EPCs) after transplantation into the rat heart (*ex vivo* myocardial tissue sections confirmed that the ^{124}I signal was linearly related to the number of EPCs present in the heart). They also showed that pretreatment of the rat with a combination of Atorvastatin and VEGF led to a prolongation of early survival of the transplanted EPCs.

NIS can also be used as a reporter gene for monitoring immune cell trafficking *in vivo*. Seo *et al.* (2010) [132] published the first study using NIS reporter gene imaging to monitor macrophage migration towards inflamed tissue [132]. These investigators used an immortalized macrophage cell line genetically engineered to express NIS and GFP (RAW264.7/hNIS-GFP) and small animal PET imaging with ^{18}F-FDG and ^{124}I to image an area of chemically-induced inflammation in a nude mouse thigh that was created by the intramuscular injection of turpentine. The rate of cell proliferation, cytokine production, and phagocytic activity were not affected by the insertion of the NIS and GFP dual reporter transgenes. PET images obtained with both ^{18}F-FDG and ^{124}I showed a similar "doughnut-shaped" area of uptake at the inflammation/injection site in the rat thigh. The migration of macrophages to this inflamed site was further confirmed by *ex vivo* IHC staining.

THE ADVANTAGES OF MICRO-SPECT AND MICRO-PET FOR NIS IMAGING IN SMALL ANIMALS

NIS-mediated transport activity *in vivo* allows the use of standard nuclear medicine imaging modalities including planar gamma-camera (scintigraphy) and single photon emission computed-tomography (SPECT) using ^{99m}TC, ^{125}I, and ^{123}I, and positron emission tomography (PET) using ^{124}I and ^{18}F-tetrafluoroborate. Prior to the development of dedicated small animal imaging systems most preclinical imaging employed large human clinical systems or laboratory instruments designed for other purposes, such as a phosphorimager. Over the past 10 years, significant advances in instrumentation and image reconstruction software have led to the development and commercialization of multiple dedicated small animal SPECT and PET systems [133-143].

Currently, planar scintigraphy is more widely available, is less expensive than cross-sectional imaging with SPECT or PET, and has been the most widely used imaging modality for preclinical NIS research. The planar gamma camera remains a useful tool because it enables the determination of the whole-body biodistribution of an injected radionuclide. In fact several small animals can be imaged simultaneously due to the large field of view afforded by the gamma camera. However, the planar gamma camera has considerable limitations due to its low resolution and because it represents a 3-D distribution of radioactivity in a 2-D display [144, 145]. This results in superimposition of overlying radioactivity, difficulty with accurate localization of abnormalities, and errors in radiotracer quantitation [146]. In addition to these general problems, there are also potential challenges with the NIS reporter for *in vivo* planar scintigraphy with radionuclide-based techniques because of high radiotracer uptake in the stomach that may result in a strong signal on the 2-D scintigraphic images. This may lead to decreased spatial resolution and inaccurate monitoring of NIS expression in adjacent abdominal organs such as the liver, spleen, and pancreas.

Cross-sectional imaging techniques such as SPECT and PET are needed to improve 3-D spatial resolution and separate the overlapping regions of radioiodine uptake *in vivo*. Combined multi-modality scanners have recently been developed that allow fusion of functional (SPECT or PET) data with high-resolution anatomical (CT) data to provide a more accurate localization and quantitative estimate of radioactivity in live animals. A tri-modal small-animal PET/SPECT/CT system was also recently introduced [141].

Although PET is more often used than SPECT for clinical applications because of its higher sensitivity, resolution, and quantitative advantages for deep-tissue imaging, this is not the case for small animal imaging. There are several excellent recent review articles comparing the advantages and disadvantages of micro-SPECT and micro-PET imaging in preclinical research [141, 143, 147-149]. Briefly, micro-SPECT and micro-PET both use similar detector systems and record the emission of photons *in vivo* to document the location of an administered radiotracer. The type of decay that each of the system detects, however, is different (single gamma photon emission for SPECT versus two photon emission from positron annihilation for PET) and therefore requires the use of different radionuclides.

Two of the biggest differences between small animal SPECT and PET are with regard to image sensitivity and resolution. SPECT imaging requires the use of a lead collimator to detect and convey information about the origin and direction of the gamma photon for representation in a 3-dimensional image format. Because lead collimators reject the majority of emitted gamma photons (>99%), the sensitivity of SPECT is approximately 2 orders of magnitude lower than PET and therefore requires higher doses of administered radiotracer and/or increased imaging time [143, 147, 148]. Cheng *et al.* (Cheng 2010) compared two commercially available small animal SPECT and PET imaging systems with regard to image sensitivity and resolution by imaging a mouse flank xenograft using $^{99m}Tc0_4$ and ^{18}F-labeled tumor-specific nanoparticles. Their results demonstrated 15-fold higher sensitivity with PET for detection of tumor radioactivity. The trade-off, however, is that SPECT can employ multiple pinhole collimators to provide higher *spatial resolution* than PET (down to < 0.5 mm for micro-SPECT versus 1 to 2 mm for micro-PET) [143, 148]. Marsee *et al.* [74] were the first to image NIS expression with micro-SPECT/CT and were able to detect NIS-expressing orthotopic lung tumors as small 3 mm with ^{125}I micro-SPECT using pinhole collimation. Newer generation micro-SPECT systems offer sub-millimeter image resolution with increased sensitivity using a detector with a larger surface area and increased field-of-view [138, 140]. Targeted pinhole micro-SPECT can also be used to increase SPECT imaging sensitivity [142] within a small field of view.

Several researchers have used ^{124}I PET imaging to document *in vivo* NIS expression [65, 71, 75, 81, 128, 150]. Groot-Wassink, *et al.* showed a strong correlation (r = 0.9581) between PET imaging quantitation (%ID/g) and *ex vivo* analysis of ^{124}I hepatic uptake in mice systemically administered a NIS-expressing adenovirus [71]. Dingli, *et al.* [81] used a clinical PET/CT scanner to document and quantitate NIS-mediated ^{124}I uptake in stable NIS-expressing (25% ID) and MV-NIS infected (7.1%) mouse myeloma xenografts. The drawbacks associated with use of ^{124}I are that it is not readily available, its production is complex, and the tissue penetration prior to annihilation of the high energy positrons from ^{124}I decay (maximum positron range of >6 mm) severely limits the spatial resolution in a small animal setting [151]. A recent breakthrough in NIS research is the development of a novel PET probe ^{18}F-tetrafluoroborate ([^{18}F]TFB) [152, 153]. Although not yet widely used, this may replace the less sensitive and lower resolution ^{124}I for PET imaging of NIS.

In addition to image sensitivity and resolution, there are several other factors to consider with regard to choosing an imaging modality for NIS. Advantages of SPECT compared to PET for small animal studies are that SPECT is 1) less expensive, 2) able to image multiple probes labeled with different radiotracers of different energies at one time allowing the visualization of more than one molecular event, 3) ability to use radiotracers that are readily available at on-site pharmacies and that do not require an on-site cyclotron for production. However, both micro-SPECT and micro-PET can provide similar highly accurate *in vivo* quantitation of radioactivity and have been thoroughly validated by direct comparison with ex-vivo analyses [71, 84, 122, 136, 143].

RELATIONSHIP BETWEEN IMAGING ACTIVITY AND FRACTION OF NIS-EXPRESSING CELLS

Ultimately the result of quantitative imaging can be viewed as a concentration (some measure of atoms or activity *per unit of mass or volume*). In molecular imaging this is often referred to as absolute quantitation. The term "absolute quantitation" helps to distinguish it from other forms of image quantitation that are relative to internal or external controls in either a spatial or temporal manner. From the concentration value obtained from imaging, with appropriate validation experiments, it is then possible to calculate the fraction or number of NIS-expressing cells within a given volume. It is important to note here that thyroid quantitation is fundamentally different in this regard. The results of quantitative thyroid image analysis are usually presented as % injected dose with no denominator. The reasons for this are 1) the ability of the thyroid to compete with all other forms of radioiodide tracer *clearance* in the body is an important physiological property of the gland, and 2) when concentration is required (such as in dosimetry calculations), a standard organ mass is often used.

In theory, both CT and SPECT (or PET) are absolutely quantitative because imaging instruments are calibrated with standards so the reconstructed CT dimensions and SPECT or PET voxel (a volumetric or three-dimensional pixel) intensity exactly match the true dimensions and true radionuclide concentration within the voxel. In humans, however, attenuation of photons and Compton scatter result in considerable loss of photons reaching the detector in comparison to instrument calibration standards where the surrounding medium is air.

In mice, with medium energy photons such as those from ^{99m}Tc decay (140 keV) or positron annihilation (511 keV), attenuation and scatter losses are minimal. However, a different impediment to accurate quantitation is encountered—the resolution of small animal micro-SPECT/CT or micro-PET/CT devices is much lower than human SPECT/CT or PET/CT relative to anatomical volume. Thus, large corrections are required for partial volume effects, where the majority of counts are projected (displayed) outside of the volume from which they emanated. With a spherical tumor of uniform activity, this partial volume effect can be corrected for based on standard curves generated from imaging spherical phantoms of known dimension and activity Fig. (**1**) [84]; however, for different shaped tumors and non-uniformly distributed signals, deviations from the standards are often too large to provide accurate quantitative data.

Additionally, at the CT settings typically employed for small animal imaging, [84, 103] even subcutaneous tumors are only weakly resolved from underlying skeletal muscle, surrounding fluid, and overlying skin. These difficulties in small animal SPECT/CT and PET/CT have resulted in a general bias where tumors for quantitative imaging studies are often much larger than those employed for therapy studies in the same model. In a recent paper [122], we attempted to address these issues by using 1) 1-mm pinhole SPECT collimation, 2) SPECT-based volume of interest (VOI) analysis, 3) empirical tumor-based CT optimization for accurate measurement of *in vivo* subcutaneous tumor dimensions, and 4) tumor volumes that are more typical of established tumor models for therapy (0.1 to 0.6 cm^3). We directly compared the *in vivo* imaging measurements to *ex vivo* measurements immediately following imaging. Fig. (**2**) Using a threshold of 1.5-fold above control tumor uptake (background), we calculated 2.7% MV-NIS-infected BxPC-3 tumor cells were required for detection within this model. Additionally, by measuring the volume of BxPC-3 tumor cells and the tumor cell/stroma ratio, we can calculate that with the imaging settings employed (2.2 mm voxel size), approximately 2 x 10^5 infected tumors cells are required to reliably resolve a zone of infection from background in this model Fig. (**3**). We have applied the same general techniques to orthotopic pancreatic tumors stably expressing NIS Fig. (**4**), and to document multiple sites of MV-NIS injection and infection within a single flank tumor Fig. (**3**).

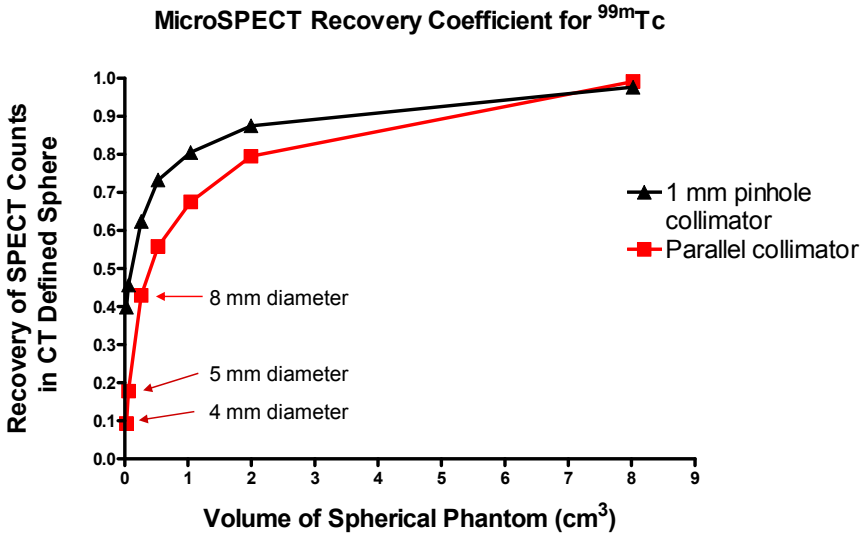

Fig. (1). A spherical phantom study to determine the partial volume losses on a Gamma-Medica (Northbridge, CA) X-SPECT System. Images for the $^{99m}TcO_4$ phantom series were obtained with a high-sensitivity parallel-hole collimator and a 1-mm pinhole collimator. The fraction of counts displayed within CT defined spheres is plotted as a function of sphere volume.

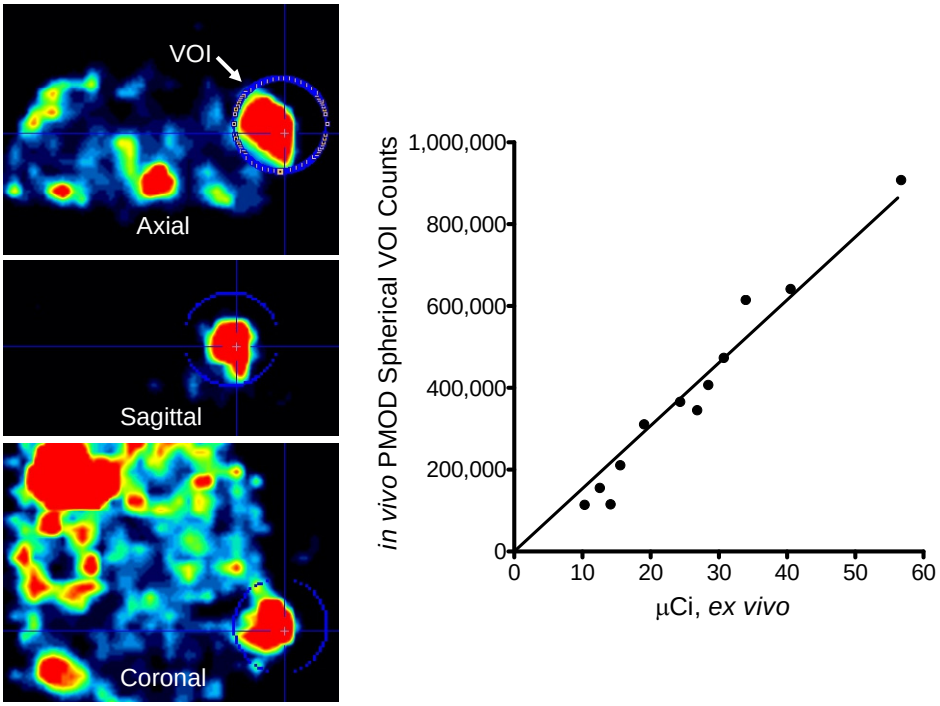

Fig. (2). Pinhole micro-SPECT/CT image analysis versus *ex vivo* quantitation of BxPC-3 tumors 3 days post-infection with an oncolytic measles virus encoding NIS. A single spherical volume of interest (VOI) was drawn around each tumor and the activity determined with PMOD imaging software. Immediately following imaging, tumors were excised and counted in a dose calibrator.

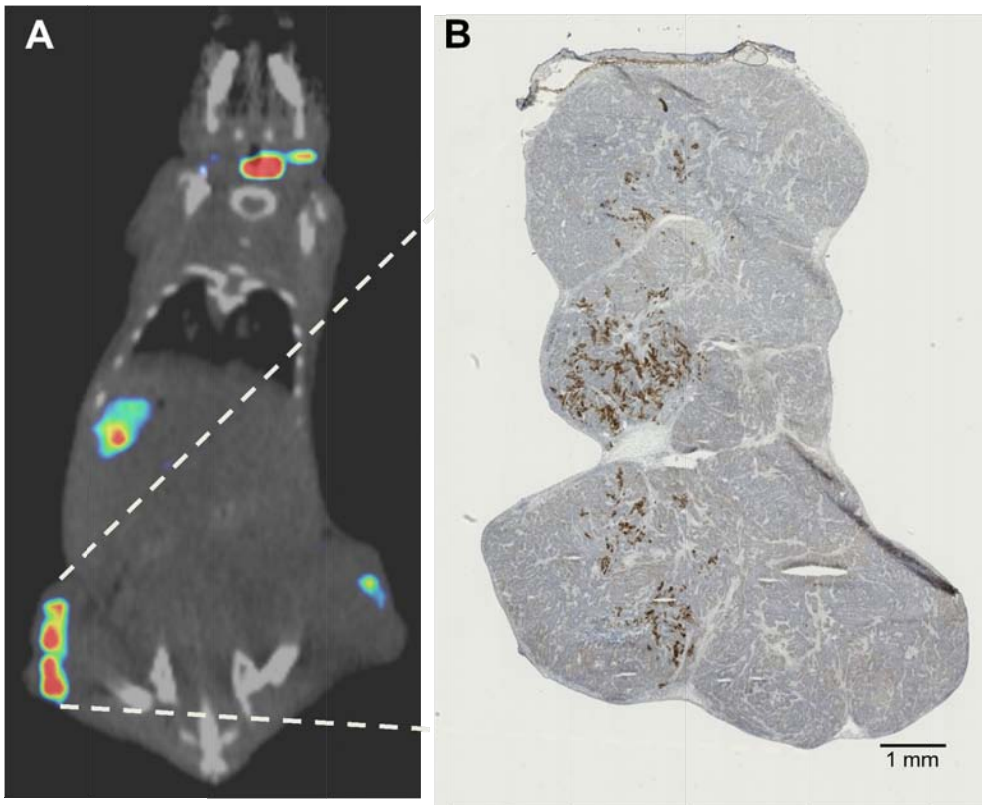

Fig. (3). Micro-SPECT/CT image and corresponding immunohistochemistry analysis of early infection with multiple intratumoral injections of MV-NIS. A BxPC-3 xenograft was injected in three locations with a total dose of 3.5 x 10^6 MV-NIS. On day 4 post-injection, the animal was imaged with pinhole micro-SPECT/CT. (**A**) The tumor was removed, aligned with the micro-SPECT/CT image, processed by IHC for measles N (brown staining), and counterstained with hematoxylin. (**B**) An excellent spatial correlation is seen between the live animal micro-SPECT/CT image and the three small zones of intratumoral infection.

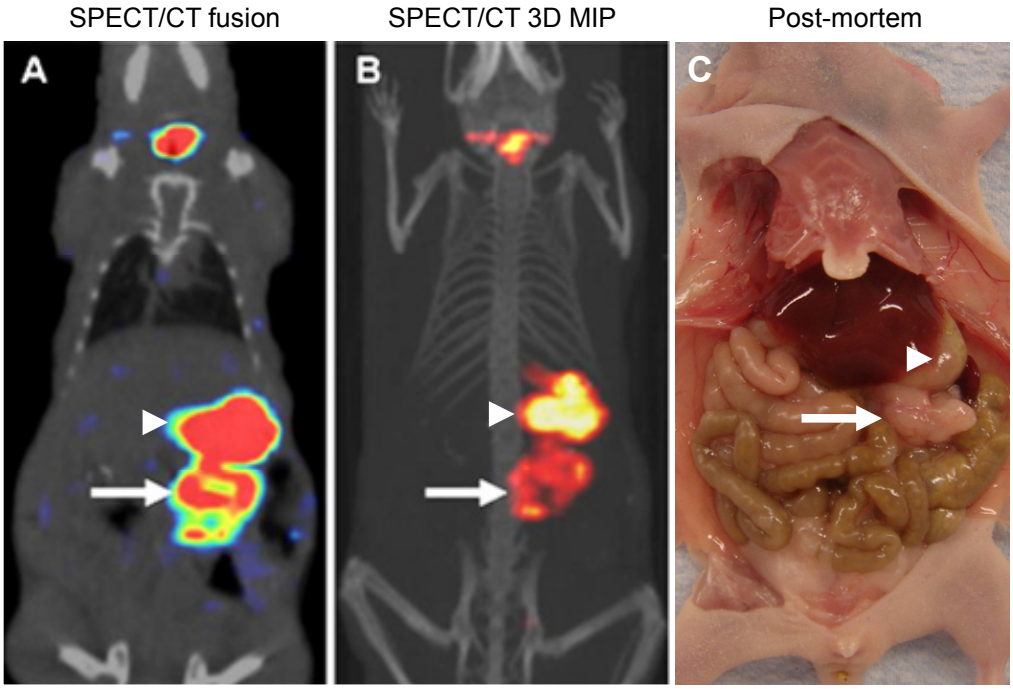

Fig. (4). Micro-SPECT/CT imaging of an orthotopic transplantation model of pancreatic cancer. BxPC-3-NIS xenograft fragments were transplanted to the pancreas of donor mice. Twenty days after transplantation, animals were injected with 1 mCi $^{99m}TcO_4$ and imaged 1 h later. (**A**) Coronal fusion micro-SPECT/CT slice through the center of the pancreatic tumor (arrow) adjacent to the endogenous stomach activity (arrowhead). Thyroid uptake is also seen on the image. (**B**) The same imaging data set is displayed as a maximum intensity projection (MIP) generated from threshold-adjusted axial slices. (**C**) Post-mortem analysis reveals the size and location of the pancreatic tumor (arrow) relative to adjacent stomach (arrowhead) and other organs.

A number of other reports have demonstrated the ability of the NIS transgene to serve as an absolute quantitative reporter for gene therapy vectors. Groot-Wassink *et al.* (2004) [71] performed a study with a non-replicating adenoviral vector expressing a CMV promoter-driven NIS (Ad-hNIS). They administered increasing doses of Ad-hNIS (5×10^6 to 2.5×10^9 pfu) to C57/B6 mice via tail vein injection. To validate the quantitative reporter aspects of the transgene, an ex-vivo comparison of NIS-mediated ^{124}I accumulation and NIS RNA (as a surrogate for infected cells) was performed. The results indicated a nearly perfect correlation between ^{124}I quantitation and NIS RNA in both the threshold dose to establish a significant infection and linearity with increasing dose above the threshold. Subsequent IHC analysis of mouse liver sections enabled an estimate of the relationship between ^{124}I concentration, quantitative RNA analysis, and percent of cells infected with virus. Further experiments were performed to confirm the *in vivo* quantitative analysis with ^{124}I PET. A nearly perfect linear correlation was confirmed between volume of interest image analysis and *ex vivo* measurements of radiotracer uptake. In this example, the liver is quite large relative to the resolution of the imaging system and a uniform distribution of IV administered Ad-hNIS within the liver can be assumed. Therefore, the conversion of imaging "activity" to a meaningful measure of absolute concentration (% ID/g) is straightforward. In a similar study, Lee and Kim *et al.* (2005) [83] assessed infection in living rats following intramyocardial injection of an adenovirus expressing NIS and eGFP [83]. As in the Groot-Wassink study, a threshold dose of Ad-GFP-NIS was required to establish a quantifiable infection. Beyond that, however, there was a very good correlation between % ID/g (following administration of ^{123}I) and the measurement of quantitative fluorescence for GFP content in the transduced cardiac tissue.

A fundamentally different form of quantitative reporter use of NIS was tested in a study by Vadysirisack *et al.* (2006) [154]. The authors attempted to determine the utility of NIS as a gene/promoter reporter. They used quantitative immunoblotting, RNA analysis, and a tetracycline-inducible promoter to drive a gradient of NIS expression. This enabled a direct comparison between NIS mRNA levels, total NIS, surface NIS, and iodide transport activity in a synchronized manner. They observed in several different cell types a level of NIS surface protein above which additional steady iodide transport activity did not occur. This non-linear relationship between NIS mRNA, NIS protein, and NIS activity, indicates that NIS is probably not an ideal candidate reporter for a gene/promoter assay.

Conditionally-replicating adenovirus (CRAds) may represent the most difficult challenge to the concept of NIS reporter quantitation of transduction. With CRAds there may be a clear virion per cell (gene dose) response at early time points or if the cells are minimally permissive to amplification. While in other cells, a region of low MOI infection combined with substantial amplification could result in a similar imaging signal as a high MOI infection. In order to deal with these practical issues, Barton *et al.*, [66, 119, 121] introduced the concept of gene expression volume (GEV, with units of cm^3) and the gene expression unit (GE, which equals the GEV times the ratio of imaging intensity in the

GEV to that of blood). For example, a region of interest signal of 1 cm^3 with a mean calculated probe concentration of 3 times that of the blood would equal 3 GE units. These units could then serve as reference values for optimization of intratumoral injections where the combined volume of NIS activity and magnitude of NIS activity should reflect the total tissue dose of drug produced from a prodrug convertase encoded in the same virus. In a phase 1 clinical trial extension, Barton *et al.* 2011 [121] used a replication-competent adenovirus encoding a yeast cytosine deaminase (yCD)--herpes simplex virus thymidine kinase (*mut*TK_{SR39}) fusion protein and a second transgene encoding NIS (Ad5-yCD/*mut*TK_{SR39}*rep*-hNIS). They directly injected 5 x 10^{12} Ad5-yCD/*mut*TK_{SR39}*rep*-hNIS viral particles divided into twelve injection sites into the prostate of 6 patients with localized prostate cancer. The patients were imaged serially with SPECT/CT after intravenous injection of $^{99m}Tc0_4$ beginning one day after administration of the virus. Quantitative SPECT/CT image analysis enabled the determination of 1) the volume of Ad5-yCD/*mut*TK_{SR39}*rep*-hNIS infected prostate, 2) the concentration of ^{99m}Tc within each GEV and it's relation to adjacent organs and blood, 3) the % of prostate infected, and the 4) the rate of disappearance of infection from the prostate.

RADIONUCLIDE BASED REPORTER/PROBE SYSTEMS

Radionuclide-based reporter imaging techniques with scintigraphy, SPECT, or PET offer the highest sensitivity for detecting low levels of reporter gene expression (picomolar sensitivity) and appear the most suited for translation to the clinic at this time [1, 2, 155, 156]. Optical imaging techniques (with bioluminescent enzyme/substrate systems or fluorescent proteins) are useful in small animals, but are limited in humans due to the depth of tissue penetration (generally < 2cm) [157]. Magnetic resonance imaging with specific contrast agents offers high spatial resolution [158-160] but is less sensitive than radionuclide techniques and is limited by the high concentration of contrast material required to provide sufficient image contrast [161].

In addition to NIS, several other radionuclide based reporter systems have been utilized for preclinical and translation studies. Table **1** contains a list of these reporter proteins, along with some of the commonly employed SPECT and PET probes for each reporter. Radiological (physical) half-life, positron yield, maximum positron energy for PET isotopes, and the principle 'imageable" gamma photon for SPECT isotopes are given for each radionuclide. Herpes simplex virus-1 thymidine kinase (TK) and an optimized mutant (*sr39tk)*, which has higher affinity for imaging probes and lower affinity for thymidine, can be imaged with radiolabeled acycloguanosines or 2'-fluoro nucleoside analogs of thymidine. The Dopamine D2 receptor (DR2) and a second generation receptor (R80A), which retains ligand binding function but does mediate internal signaling, can be imaged with ^{11}C, ^{18}F, or ^{123}I-labeled D2 antagonists. Likewise, a variety of somatostatin analogs are available for either PET or SPECT imaging of the somatostatin receptor type 2 (SSRT2). The norepinephrine transporter (NET) can be imaged with either ^{123}I or ^{124}I MIBG (a norepinephrine analog). Radionuclide probes for NIS are either radioactive isotopes of iodide (^{123}I, ^{124}I, ^{125}I), or molecules with a size and charge density similar to iodide, such as $^{99m}Tc0_4$ or [^{18}F]-TFB.

NIS VERSUS OTHER SPECT/PET REPORTERS

As can be seen in Table **1**, all of the commonly employed radionuclide reporters can be imaged with either PET or SPECT probes. Thus, the decision to choose one reporter or another can be made largely upon biological considerations rather than on the basis of instrumentation. Some biological considerations when choosing a reporter/probe system are (1) endogenous receptor activity, background localization of probe, location of target tissue in relation to regions of high probe concentration, and the timing and potential competition of endogenous activity and background in relation to the desired reporter signal. In this regard, NIS would not be desirable for a reporter in the stomach or bladder. However, the low background of NIS probe activity in liver, kidney, or skeletal muscle for example might be ideal for NIS imaging. (2) For conventional gene therapy approaches, it is desirable to use a self-protein as a reporter to minimize the possibility of immune-mediated destruction of cells encoding the reporter. An advantage of NIS is this regard is that in addition to being a self-protein, NIS-encoding constructs from several species including mouse, rat, human, and dog (Stephen J. Russell, unpublished), have been developed and tested in animals. (3) Also, for conventional gene therapy, it is important to consider biological activity of the ectopically expressed reporter and its effect on cell physiology (either constitutive activity or through the action of endogenous substrates). These issues have been addressed for HSV-1 TK and D2R with the engineering of vectors encoding the *sr39tk* mutant and R80A mutant, respectively [155, 162]. Theoretically, constitutive activity might be a concern for NIS. However, long term culturing of stable NIS expressing cells lines, as well as long term expression of NIS in normal animal tissue, for example, in the NIS transgenic heart mouse [163], would seem to indicate that most cells are quite able to tolerate a background level of NIS activity. (4) A final biological consideration is the size of the reporter gene—the vector must be able to accommodate the insert. In this respect, NIS is the largest of the reporters, which could limit its applications in some viruses with strict limits on insert size.

If these biological considerations above are met, the primary advantage of NIS is that it can be used with inexpensive and readily available $^{99m}TcO_4$. $^{99m}TcO_4$ costs only a few dollars per dose and can be eluted daily from an in-house generator. No labeling reactions are required, and the imaging characteristics (140 keV gamma) are ideal and standardized for quantitative SPECT/CT imaging in both small animal and human instruments. A disadvantage of NIS versus some other commonly employed reporters is that the only approved PET isotope for NIS imaging is ^{124}I. The high energy positrons released from ^{124}I decay have a long range in tissue prior to annihilation, which limits resolution, and the yield of positrons from ^{124}I is quite low relative to several other PET isotopes [164-166]. It remains to be seen if [^{18}F]-TFB will be approved for human use. However, if approved, [^{18}F]-TFB should provide the ideal combination of sensitivity (four ^{18}F atoms per molecule) and resolution for PET imaging of the NIS reporter.

Table 1. Heterologous Reporter/Probe Imaging Strategies

Reporter	Probe	Modality	Half-life	Positron (yield), Energy	References
Dopamine D2 Receptor (R80A) 443 aa	[^{11}C]raclopride	PET	20 min	β^+ (100%), 0.96 MeV	[162, 167-171]
	3-(2′-[^{18}F]fluoroethyl)-spiperone	PET	110 min	β^+ (97%), 0.635 MeV	
	[^{123}I]iodobenzamine	SPECT	13.3 h	γ, 159 keV	
Herpes Simplex Virus-1 Thymidine Kinase (sr39tk) 376 aa	9-[4-[^{18}F]fluoro-3-(hydroxymethyl)butyl] guanine ([^{18}F]FHBG)	PET	110 min	β^+ (97%), 0.635 MeV	[77, 155, 172-180]
	1-(2-deoxy-2-[^{18}F]fluoro-D-arabinofuranosyl)-5-iodouracil ([^{18}F]FIAU)	PET	110 min	β^+ (97%), 0.635 MeV	
	1-(2-deoxy-2-fluoro-D-arabinofuranosyl)-5-[^{124}I]iodouracil([^{124}I]FIAU)	PET	4.2 days	β^+ (25%), 2.13 MeV	
	[^{125}I]FIAU	SPECT	59 days	γ, 35 keV	
	[^{18}F]-2′-Fluoro-2′deoxy-1h-D-arabionofuranosyl-5-ethyl-uracil ([^{18}F]FEAU)	PET	110 min	β^+ (97%), 0.635 MeV	
Somatostatin Receptor Type 2 369 aa	^{111}In-octreotide	SPECT	2.8 days	γ, 171, 245 keV	[181-186]
	^{99m}Tc-octreotide	SPECT	6 h	γ, 144 keV	
	^{68}Ga-dotatate	PET	68 min	β^+ (90%), 1.90 MeV	
	^{94m}Tc-demotate-1	PET	53 min	β^+ (72%), 2.47 MeV	
Norepinephrine Transporter 617 aa	meta[^{123}I]iodobenzyl-guanidine ([^{123}I]MIBG)	SPECT	13.3 h	γ, 159 keV	[187-190]
	meta[^{124}I]iodobenzyl-guanidine ([^{124}I]MIBG)	PET	4.2 days	β^+ (25%), 2.13 MeV	
Sodium Iodide Symporter 643 aa	$^{99m}Tc0_4$	SPECT	6 h	γ, 140 keV	[55, 59, 60, 62, 65, 152, 153, 191]
	^{123}I	SPECT	13.3 h	γ, 159 keV	
	^{125}I	SPECT	59 days	γ, 35 keV	
	^{124}I	PET	4.2 days	β^+ (25%) 2.13 MeV	
	[^{18}F]tetrafluoroborate	PET	110 min	β^+ (97%), 0.635 MeV	

Legend: R80A refers to Arg to Ala substitution at residue 80;

sr39tk is a thymidine kinase mutant with increased activity against acycloguanosines;

γ, gamma photon, β^+, positron.

CONCLUSIONS

As indicated throughout this review, the desirable attributes of NIS are its quantitative nature, its remarkable flexibility of iodide transport activity in many cells types using viral and non-viral platforms, and the ease in which the activity is observed *in vivo*. The main hurdle to the use of NIS transgene and all other reporter-based technology is the sensitivity (the concentration of probe within the target region versus that in the plasma or neighboring region). Sensitivity is of particular concern for oncolytic virotherapy research using replicating viruses where it is desirable to detect lower levels of infection that may cause unwanted side effects, and for situations where the goal is to obtain "proof of concept" information in a model that may not be a "best case scenario". The hope is that with continued work in basic research to improve sensitivity, validation in relevant animal models, and ultimately translation to human clinical trials, we will see a time when the concept of imaging reporter-guided gene therapy, viral therapy, and cell-based therapy becomes a standard of care for diseases which today are untreatable.

Additionally there is hope that in the future reporter gene imaging will facilitate more than simply accurate reporting on the spatial and temporal pattern of vectors. It is conceivable that the results of reporter imaging will both serve as a guide for confirmatory biopsies and enable clinicians to make rational decisions about additional or complementary therapies on a patient-by-patient basis

CONFLICT OF INTEREST

Declared none.

ACKNOWLEDGEMENTS

The authors would like to thank Dr. Claire Bender and Kelly Classic for helpful discussion and thorough review of the article draft.

REFERENCES

[1] Serganova I, Mayer-Kukuck P, Huang R, Blasberg R. Molecular imaging: reporter gene imaging. Handb Exp Pharmacol [Review] 2008; (185 Pt 2): 167-223.

[2] Waerzeggers Y, Monfared P, Viel T, Winkeler A, Voges J, Jacobs AH. Methods to monitor gene therapy with molecular imaging. Methods. [Research Support, Non-U.S. Gov't Review]. 2009; 48(2): 146-60.

[3] Carrasco N. Iodide transport in the thyroid gland. Biochim Biophys Acta 1993 Jun 8;1154(1):65-82.

[4] Spitzweg C, Heufelder AE, Morris JC. Thyroid iodine transport. Thyroid : official journal of the American Thyroid Association [Review] 2000; 10(4): 321-30.

[5] De La Vieja A, Dohan O, Levy O, Carrasco N. Molecular analysis of the sodium/iodide symporter: impact on thyroid and extrathyroid pathophysiology. Physiol Rev [Research Support, Non-U.S. Gov't Research Support, U.S. Gov't, P.H.S. Review] 2000; 80(3): 1083-105.

[6] Spitzweg C, Harrington KJ, Pinke LA, Vile RG, Morris JC. Clinical review 132: The sodium iodide symporter and its potential role in cancer therapy. J Clin Endocrinol Metab 2001; 86(7): 3327-35.

[7] Cho JY. A transporter gene (sodium iodide symporter) for dual purposes in gene therapy: imaging and therapy. Curr Gene Ther [Review] 2002; 2(4): 393-402.

[8] Spitzweg C, Morris JC. The sodium iodide symporter: its pathophysiological and therapeutic implications. Clin Endocrinol (Oxf) [Research Support, Non-U.S. Gov't Review] 2002; 57(5): 559-74.

[9] Chung JK. Sodium iodide symporter: its role in nuclear medicine. J Nucl Med 2002; 43(9): 1188-200.

[10] Dohan O, De la Vieja A, Paroder V, *et al.*. The sodium/iodide Symporter (NIS): characterization, regulation, and medical significance. Endocr Rev. [Research Support, Non-U.S. Gov't Research Support, U.S. Gov't, Non-P.H.S. Research Support, U.S. Gov't, P.H.S. Review] 2003; 24(1): 48-77.

[11] Elisei R, Vivaldi A, Pacini F. Biology and clinical application of the NIS gene. Tumori. [Review] 2003; 89(5): 523-8.

[12] Dingli D, Russell SJ, Morris JC, 3rd. *In vivo* imaging and tumor therapy with the sodium iodide symporter. J Cell Biochem 2003; 90(6): 1079-86.

[13] Dadachova E, Carrasco N. The Na/I symporter (NIS): imaging and therapeutic applications. Semin Nucl Med [Review] 2004; 34(1): 23-31.

[14] Baker CH, Morris JC. The sodium-iodide symporter. Curr Drug Targets Immune Endocr Metabol Disord 2004; 4(3): 167-74.

[15] Riesco-Eizaguirre G, Santisteban P. A perspective view of sodium iodide symporter research and its clinical implications. Eur J Endocrinol. [Research Support, Non-U.S. Gov't Review] 2006; 155(4): 495-512.

[16] Baril P, Martin-Duque P, Vassaux G. Visualization of gene expression in the live subject using the Na/I symporter as a reporter gene: applications in biotherapy. Br J Pharmacol [Research Support, Non-U.S. Gov't Review] 2010; 159(4): 761-71.

[17] Hingorani M, Spitzweg C, Vassaux G, *et al.*. The biology of the sodium iodide symporter and its potential for targeted gene delivery. Curr Cancer Drug Targets 2010; 10(2): 242-67.

[18] Chung JK, Kang JH. Translational research using the sodium/iodide symporter in imaging and therapy. Eur J Nucl Med Mol Imaging 2004; 31: 799-802.

[19] Smith VE, Franklyn JA, McCabe CJ. Expression and function of the novel proto-oncogene PBF in thyroid cancer: a new target for augmenting radioiodine uptake. J Endocrinol [Research Support, Non-U.S. Gov't Review] 2011; 210(2): 157-63.

[20] Czarnocka B. Thyroperoxidase, thyroglobulin, Na(+)/I(-) symporter, pendrin in thyroid autoimmunity. Front Biosci [Research Support, Non-U.S. Gov't Review] 2011; 16: 783-802.

[21] Leung AM, Pearce EN, Braverman LE. Perchlorate, iodine and the thyroid. Best Pract Res Clin Endocrinol Metab [Review] 2010; 24(1): 133-41.

[22] O'Neill CJ, Oucharek J, Learoyd D, Sidhu SB. Standard and emerging therapies for metastatic differentiated thyroid cancer. Oncologist 2010; 15(2): 146-56.

[23] Spitzweg C, Morris JC. Genetics and phenomics of hypothyroidism and goiter due to NIS mutations. Mol Cell Endocrinol 2010; 322(1-2): 56-63.

[24] Yen PM. Physiological and molecular basis of thyroid hormone action. Physiol Rev 2001; 81(3): 1097-142.

[25] Szkudlinski MW, Fremont V, Ronin C, Weintraub BD. Thyroid-stimulating hormone and thyroid-stimulating hormone receptor structure-function relationships. Physiol Rev 2002; 82(2): 473-502.

[26] Pohlenz J, Refetoff S. Mutations in the sodium/iodide symporter (NIS) gene as a cause for iodide transport defects and congenital hypothyroidism. Biochimie 1999; 81(5): 469-76.

[27] Bizhanova A, Kopp P. Minireview: The sodium-iodide symporter NIS and pendrin in iodide homeostasis of the thyroid. Endocrinology 2009; 150(3): 1084-90.

[28] Schlumberger M, Lacroix L, Russo D, Filetti S, Bidart JM. Defects in iodide metabolism in thyroid cancer and implications for the follow-up and treatment of patients. Nat Clin Pract Endocrinol Metab 2007; 3(3): 260-9.

[29] Wang ZF, Liu QJ, Liao SQ, *et al.*. Expression and correlation of sodium/iodide symporter and thyroid stimulating hormone receptor in human thyroid carcinoma. Tumori 2011; 97(4): 540-6.

[30] Huang H, Shi Y, Lin L, *et al.*. Intracellular iodinated compounds affect sodium iodide symporter expression through TSH-mediated signaling pathways. Mol Med Report 2011; 4(1): 77-80.

[31] Harun-Or-Rashid M, Asai M, Sun XY, Hayashi Y, Sakamoto J, Murata Y. Effect of thyroid statuses on sodium/iodide symporter (NIS) gene expression in the extrathyroidal tissues in mice. Thyroid Res 2010; 3(1): 3.

[32] Serrano-Nascimento C, Calil-Silveira J, Nunes MT. Posttranscriptional regulation of sodium-iodide symporter mRNA expression in the rat thyroid gland by acute iodide administration. Am J Physiol Cell Physiol 2010; 298(4): C893-9.

[33] Hou P, Bojdani E, Xing M. Induction of thyroid gene expression and radioiodine uptake in thyroid cancer cells by targeting major signaling pathways. J Clin Endocrinol Metab 2010; 95(2): 820-8.

[34] Hays MT, Berman M. Pertechnetate distribution in man after intravenous infusion: a compartmental model. J Nucl Med 1977; 18(9): 898-904.

[35] Hays MT. Kinetics of the human thyroid trap: a compartmental model. J Nucl Med 1978; 19(7): 789-95.

[36] Hays MT. Kinetics of the human thyroid trap: effects of iodide, thyrotropin, and propylthiouracil. J Nucl Med 1979; 20(9): 944-9.

[37] Valenta L. Metastatic thyroid carcinoma in man concentrating iodine without organification. J Clin Endocrinol Metab 1966; 26(12): 1317-24.

[38] Steinberg M, Cavalieri RR, Choy SH. Uptake of technetium 99-pertechnetate in a primary thyroid carcinoma: need for caution in evaluating nodules. J Clin Endocrinol Metab 1970; 31(1): 81-4.

[39] Usher MS, Arzoumanian AY. Thyroid nodule scans made with pertechnetate and iodine may give inconsistent results. J Nucl Med 1971; 12(3): 136-7.

[40] Schall GL, Roth JA, Temple R. Differential uptake of 125 I - and 99m TcO 4 - in a histologically unusual metastatic thyroid carcinoma. J Surg Oncol 1973; 5(3): 235-42.

[41] Shambaugh GE, 3rd, Quinn JL, Oyasu R, Freinkel N. Disparate thyroid imaging. Combined studies with sodium pertechnetate Tc 99m and radioactive iodine. Jama 1974; 228(7): 866-9.

[42] Hirabayashi S, Koga Y, Kitachara T, Hishida T, Kiga M. Inconsistent images of thyroid nodule scintigrams made with iodine and pertechnetate: case report. J Nucl Med 1975; 16(10): 918.

[43] Turner JW, Spencer RP. Thyroid carcinoma presenting as a pertechnetate "hot" nodule, but without 131I uptake: case report. J Nucl Med 1976; 17(1): 22-3.

[44] Reschini E, Ferrari C, Castellani M, *et al.*. The trapping-only nodules of the thyroid gland: prevalence study. Thyroid 2006; 16(8): 757-62.

[45] Tazebay UH, Wapnir IL, Levy O, *et al.*. The mammary gland iodide transporter is expressed during lactation and in breast cancer. Nat Med 2000; 6(8): 871-8.

[46] Josefsson M, Grunditz T, Ohlsson T, Ekblad E. Sodium/iodide-symporter: distribution in different mammals and role in entero-thyroid circulation of iodide. Acta Physiol Scand 2002; 175(2): 129-37.

[47] Nicola JP, Basquin C, Portulano C, Reyna-Neyra A, Paroder M, Carrasco N. The Na+/I- symporter mediates active iodide uptake in the intestine. Am J Physiol Cell Physiol 2009; 296(4): C654-62.

[48] Spitzweg C, Dutton CM, Castro MR, *et al.*. Expression of the sodium iodide symporter in human kidney. Kidney Int 2001; 59(3): 1013-23.

[49] Beasley TM, Palmer HE, Nelp WB. Distribution and excretion of technetium in humans. Healthy Physics Pergamon Press 1966; 12: 1425-35.

[50] Russo D, Scipioni A, Durante C, *et al.*. Expression and localization of the sodium/iodide symporter (NIS) in testicular cells. Endocrine 2011; 40(1): 35-40.

[51] Spitzweg C, Joba W, Eisenmenger W, Heufelder AE. Analysis of human sodium iodide symporter gene expression in extrathyroidal tissues and cloning of its complementary deoxyribonucleic acids from salivary gland, mammary gland, and gastric mucosa. J Clin Endocrinol Metab 1998; 83(5): 1746-51.

[52] Vayre L, Sabourin JC, Caillou B, Ducreux M, Schlumberger M, Bidart JM. Immunohistochemical analysis of Na+/I- symporter distribution in human extra-thyroidal tissues. Eur J Endocrinol 1999; 141: 382-6.

[53] Spitzweg C, Joba W, Schriever K, Goellner JR, Morris JC, Heufelder AE. Analysis of human sodium iodide symporter immunoreactivity in human exocrine glands. J Clin Endocrinol Metab 1999; 84(11): 4178-84.

[54] Hays MT. 99m Tc-pertechnetate transport in man: absorption after subcutaneous and oral administration; secretion into saliva and gastric juice. J Nucl Med 1973; 14(6): 331-5.

[55] Boland A, Ricard M, Opolon P, *et al.*. Adenovirus-mediated transfer of the thyroid sodium/iodide symporter gene into tumors for a targeted radiotherapy. Cancer Res 2000; 60(13): 3484-92.

[56] Dai G, Levy O, Carrasco N. Cloning and characterization of the thyroid iodide transporter. Nature 1996; 379(6564): 458-60.

[57] Smanik PA, Liu Q, Furminger TL, *et al.*. Cloning of the human sodium lodide symporter. Biochem Biophys Res Commun 1996; 226(2): 339-45.

[58] Pinke LA, Dean DS, Bergert ER, Spitzweg C, Dutton CM, Morris JC. Cloning of the mouse sodium iodide symporter. Thyroid 2001; 11(10): 935-9.

[59] Shimura H, Haraguchi K, Miyazaki A, Endo T, Onaya T. Iodide uptake and experimental 131 therapy in transplanted undifferentiated thyroid cancer cells expressing the Na+/I-symporter gene. Endocrinology 1997; 138(10): 4493-6.

[60] Mandell RB, Mandell LZ, Link CJ, Jr. Radioisotope concentrator gene therapy using the sodium/iodide symporter gene. Cancer Res 1999; 59(3): 661-8.

[61] Nakamoto Y, Saga T, Misaki T, *et al.*. Establishment and characterization of a breast cancer cell line expressing Na+/I-symporters for radioiodide concentrator gene therapy. J Nucl Med 2000; 41(11): 1898-904.

[62] Spitzweg C, O'Connor MK, Bergert ER, Tindall DJ, Young CY, Morris JC. Treatment of prostate cancer by radioiodine therapy after tissue-specific expression of the sodium iodide symporter. Cancer Res 2000; 60(22): 6526-30.

[63] Haberkorn U, Henze M, Altmann A, *et al.*. Transfer of the human NaI symporter gene enhances iodide uptake in hepatoma cells. J Nucl Med 2001; 42(2): 317-25.

[64] Spitzweg C, Dietz AB, O'Connor MK, *et al.*. *In vivo* sodium iodide symporter gene therapy of prostate cancer. Gene Ther 2001; 8(20): 1524-31.

[65] Groot-Wassink T, Aboagye EO, Glaser M, Lemoine NR, Vassaux G. Adenovirus biodistribution and noninvasive imaging of gene expression *in vivo* by positron emission tomography using human sodium/iodide symporter as reporter gene. Hum Gene Ther 2002; 13(14): 1723-35.

[66] Barton KN, Tyson D, Stricker H, *et al.*. GENIS: gene expression of sodium iodide symporter for noninvasive imaging of gene therapy vectors and quantification of gene expression *in vivo*. Mol Ther 2003; 8(3): 508-18.

[67] Dingli D, Diaz RM, Bergert ER, O'Connor MK, Morris JC, Russell SJ. Genetically targeted radiotherapy for multiple myeloma. Blood 2003; 102(2): 489-96.

[68] Haberkorn U, Kinscherf R, Kissel M, *et al.*. Enhanced iodide transport after transfer of the human sodium iodide symporter gene is associated with lack of retention and low absorbed dose. Gene Ther 2003; 10(9): 774-80.

[69] Dingli D, Peng KW, Harvey ME, *et al.*. Image-guided radiovirotherapy for multiple myeloma using a recombinant measles virus expressing the thyroidal sodium iodide symporter. Blood 2004; 103(5): 1641-6.

[70] Faivre J, Clerc J, Gerolami R, *et al.*. Long-term radioiodine retention and regression of liver cancer after sodium iodide symporter gene transfer in wistar rats. Cancer Res 2004; 64(21): 8045-51.

[71] Groot-Wassink T, Aboagye EO, Wang Y, Lemoine NR, Reader AJ, Vassaux G. Quantitative imaging of Na/I symporter transgene expression using positron emission tomography in the living animal. Mol Ther 2004; 9(3): 436-42.

[72] Haberkorn U, Beuter P, Kubler W, *et al.*. Iodide kinetics and dosimetry *in vivo* after transfer of the human sodium iodide symporter gene in rat thyroid carcinoma cells. J Nucl Med 2004; 45(5): 827-33.

[73] Kang JH, Chung JK, Lee YJ, *et al.*. Establishment of a human hepatocellular carcinoma cell line highly expressing sodium iodide symporter for radionuclide gene therapy. J Nucl Med 2004; 45(9): 1571-6.

[74] Marsee DK, Shen DH, MacDonald LR, *et al.*. Imaging of metastatic pulmonary tumors following NIS gene transfer using single photon emission computed tomography. Cancer Gene Ther 2004; 11(2): 121-7.

[75] Niu G, Gaut AW, Ponto LL, *et al.*. Multimodality noninvasive imaging of gene transfer using the human sodium iodide symporter. J Nucl Med 2004; 45(3): 445-9.

[76] Shen DH, Marsee DK, Schaap J, *et al.*. Effects of dose, intervention time, and radionuclide on sodium iodide symporter (NIS)-targeted radionuclide therapy. Gene Ther 2004; 11(2): 161-9.

[77] Shin JH, Chung JK, Kang JH, *et al.*. Feasibility of sodium/iodide symporter gene as a new imaging reporter gene: comparison with HSV1-tk. Eur J Nucl Med Mol Imaging 2004; 31(3): 425-32.

[78] So MK, Kang JH, Chung JK, *et al.*. *In vivo* imaging of retinoic acid receptor activity using a sodium/iodide symporter and luciferase dual imaging reporter gene. Mol Imaging 2004; 3(3): 163-71.

[79] Yang HS, Lee H, Kim SJ *et al.*. Imaging of human sodium-iodide symporter gene expression mediated by recombinant adenovirus in skeletal muscle of living rats. Eur J Nucl Med Mol Imaging 2004; 31(9): 1304-11.

[80] Che J, Doubrovin M, Serganova I, Ageyeva L, Zanzonico P, Blasberg R. hNIS-IRES-eGFP dual reporter gene imaging. Mol Imaging 2005; 4(2): 128-36.

[81] Dingli D, Peng KW, Harvey ME, *et al.*. Interaction of measles virus vectors with Auger electron emitting radioisotopes. Biochem Biophys Res Commun 2005 ; 337(1): 22-9.

[82] Dwyer RM, Bergert ER, O'Connor M K, Gendler SJ, Morris JC. *In vivo* radioiodide imaging and treatment of breast cancer xenografts after MUC1-driven expression of the sodium iodide symporter. Clin Cancer Res 2005; 11(4): 1483-9.

[83] Lee KH, Kim HK, Paik JY, *et al.*. Accuracy of myocardial sodium/iodide symporter gene expression imaging with radioiodide: evaluation with a dual-gene adenovirus vector. J Nucl Med 2005; 46(4): 652-7.

[84] Carlson SK, Classic KL, Hadac EM, *et al.*. *In vivo* quantitation of intratumoral radioisotope uptake using micro-single photon emission computed tomography/computed tomography. Mol Imaging Biol 2006; 8(6): 324-32.

[85] Chen L, Altmann A, Mier W, *et al.*. Radioiodine therapy of hepatoma using targeted transfer of the human sodium/iodide symporter gene. J Nucl Med 2006; 47(5): 854-62.

[86] Dwyer RM, Bergert ER, O'Connor MK, Gendler SJ, Morris JC. Adenovirus-mediated and targeted expression of the sodium-iodide symporter permits *in vivo* radioiodide imaging and therapy of pancreatic tumors. Hum Gene Ther 2006; 17(6): 661-8.

[87] Dwyer RM, Bergert ER, O'Connor MK, Gendler SJ, Morris JC. Sodium iodide symporter-mediated radioiodide imaging and therapy of ovarian tumor xenografts in mice. Gene Ther 2006; 13(1): 60-6.

[88] Hasegawa K, Pham L, O'Connor MK, Federspiel MJ, Russell SJ, Peng KW. Dual therapy of ovarian cancer using measles viruses expressing carcinoembryonic antigen and sodium iodide symporter. Clin Cancer Res 2006; 12(6): 1868-75.

[89] Mitrofanova E, Unfer R, Vahanian N, Link C. Rat sodium iodide symporter allows using lower dose of 131I for cancer therapy. Gene Ther 2006; 13(13): 1052-6.

[90] Chen C-Y, Chang P-J, Changlai S-P, Pan L-K. Effective Half Life of Iodine for Five Thyroidectomy Patients Using an *in vivo* Gamma Camera Approach. J Radiat Res 2007; 48(6): 485-93.

[91] Goel A, Carlson SK, Classic KL, *et al.*. Radioiodide imaging and radiovirotherapy of multiple myeloma using VSV(Delta51)-NIS, an attenuated vesicular stomatitis virus encoding the sodium iodide symporter gene. Blood 2007; 110(7): 2342-50.

[92] Merron A, Peerlinck I, Martin-Duque P, *et al.*. SPECT/CT imaging of oncolytic adenovirus propagation in tumours *in vivo* using the Na/I symporter as a reporter gene. Gene Ther 2007; 14(24): 1731-8.

[93] Schipper ML, Riese CG, Seitz S, *et al.*. Efficacy of 99mTc pertechnetate and 131I radioisotope therapy in sodium/iodide symporter (NIS)-expressing neuroendocrine tumors *in vivo*. Eur J Nucl Med Mol Imaging. 2007; 34(5): 638-50.

[94] Siddiqui F, Barton KN, Stricker HJ, *et al.*. Design considerations for incorporating sodium iodide symporter reporter gene imaging into prostate cancer gene therapy trials. Hum Gene Ther 2007; 18(4): 312-22.

[95] Spitzweg C, Baker CH, Bergert ER, O'Connor MK, Morris JC. Image-guided radioiodide therapy of medullary thyroid cancer after carcinoembryonic antigen promoter-targeted sodium iodide symporter gene expression. Hum Gene Ther 2007; 18(10): 916-24.

[96] Willhauck MJ, Sharif Samani BR, Gildehaus FJ, *et al.*. Application of 188rhenium as an alternative radionuclide for treatment of prostate cancer after tumor-specific sodium iodide symporter gene expression. J Clin Endocrinol Metab 2007; 92(11): 4451-8.

[97] Barton KN, Stricker H, Brown SL, *et al.*. Non-Invasive, Quantitative Imaging of Adenovirus-Mediated Gene Expression in Humans with Prostate Cancer. American Society of Gene Therapy 11th Annual Meeting; May 30, 2008; Boston, Massachusetts: American Society of Gene Therapy; 2008.

[98] Herve J, Cunha AS, Liu B, *et al.*. Internal radiotherapy of liver cancer with rat hepatocarcinoma-intestine-pancreas gene as a liver tumor-specific promoter. Hum Gene Ther 2008; 19(9): 915-26.

[99] Kim SH, Chung HK, Kang JH, *et al.*. Tumor-targeted radionuclide imaging and therapy based on human sodium iodide symporter gene driven by a modified telomerase reverse transcriptase promoter. Hum Gene Ther2008 Sep; 19(9): 951-7.

[100] Park SY, Kwak W, Tapha N, *et al.*. Combination therapy and noninvasive imaging with a dual therapeutic vector expressing MDR1 short hairpin RNA and a sodium iodide symporter. J Nucl Med 2008; 49: 1480-8.

[101] Willhauck MJ, Sharif Samani BR, Klutz K, *et al.*. Alpha-fetoprotein promoter-targeted sodium iodide symporter gene therapy of hepatocellular carcinoma. Gene Ther 2008; 15(3): 214-23.

[102] Yeom CJ, Chung JK, Kang JH, *et al.*. Visualization of hypoxia-inducible factor-1 transcriptional activation in C6 glioma using luciferase and sodium iodide symporter genes. J Nucl Med 2008; 49(9): 1489-97.

[103] Carlson SK, Classic KL, Hadac EM, *et al.*. Quantitative molecular imaging of viral therapy for pancreatic cancer using an engineered measles virus expressing the sodium-iodide symporter reporter gene. AJR Am J Roentgenol 2009; 192(1): 279-87.

[104] Msaouel P, Iankov ID, Allen C, *et al.*. Noninvasive imaging and radiovirotherapy of prostate cancer using an oncolytic measles virus expressing the sodium iodide symporter. Mol Ther 2009; 17(12): 2041-8.

[105] Pham L, Nakamura T, Gabriela Rosales A, *et al.*. Concordant activity of transgene expression cassettes inserted into E1, E3 and E4 cloning sites in the adenovirus genome. J Gene Med 2009; 11(3): 197-206.

[106] Merron A, Baril P, Martin-Duque P, *et al.*. Assessment of the Na/I symporter as a reporter gene to visualize oncolytic adenovirus propagation in peritoneal tumours. Eur J Nucl Med Mol Imaging 2010; 37(7): 1377-85.

[107] Endo T, Shimura H, Saito T, Onaya T. Cloning of malignantly transformed rat thyroid (FRTL) cells with thyrotropin receptors and their growth inhibition by 3',5'-cyclic adenosine monophosphate. Endocrinology 1990; 126(3): 1492-7.

[108] Dingli D, Bergert ER, Bajzer Z, O'Connor M K, Russell SJ, Morris JC. Dynamic iodide trapping by tumor cells expressing the thyroidal sodium iodide symporter. Biochem Biophys Res Commun 2004; 325(1): 157-66.

[109] Spitzweg C, Morris JC. Gene therapy for thyroid cancer: current status and future prospects. Thyroid : official journal of the American Thyroid Association 2004; 14(6): 424-34.

[110] Miyagawa M, Beyer M, Wagner B, *et al.*. Cardiac reporter gene imaging using the human sodium/iodide symporter gene. Cardiovasc Res 2005; 65(1): 195-202.

[111] Rao VP, Miyagi N, Ricci D, *et al.*. Sodium iodide symporter (hNIS) permits molecular imaging of gene transduction in cardiac transplantation. Transplantation 2007; 84(12): 1662-6.

[112] Ricci D, Mennander AA, Pham LD, *et al.*. Non-invasive radioiodine imaging for accurate quantitation of NIS reporter gene expression in transplanted hearts. Eur J Cardiothorac Surg 2008; 33(1): 32-9.

[113] Russell SJ, Peng KW. Viruses as anticancer drugs. Trends Pharmacol Sci 2007; 28(7): 326-33.

[114] Kelly E, Russell SJ. History of oncolytic viruses: genesis to genetic engineering. Molecular Therapy 2007; 15(4): 651-9.

[115] Stanford MM, Bell JC, Vaha-Koskela MJ. Novel oncolytic viruses: riding high on the next wave? Cytokine Growth Factor Rev 2010; 21(2-3): 177-83.

[116] Breitbach CJ, Reid T, Burke J, Bell JC, Kirn DH. Navigating the clinical development landscape for oncolytic viruses and other cancer therapeutics: no shortcuts on the road to approval. Cytokine Growth Factor Rev 2010; 21(2-3): 85-9.

[117] Yamamoto M, Curiel DT. Current issues and future directions of oncolytic adenoviruses. Mol Ther 2010; 18(2): 243-50.

[118] Kirn DH. Redemption for the field of oncolytic virotherapy. Mol Ther 2011 Apr; 19(4): 627-8.

[119] Barton KN, Freytag SO, Nurushev T, *et al.*. A model for optimizing adenoviral delivery in human cancer gene therapy trials. Hum Gene Ther 2007; 18(6): 562-72.

[120] Barton KN, Stricker H, Brown SL, *et al.*. Phase I study of noninvasive imaging of adenovirus-mediated gene expression in the human prostate. Mol Ther 2008; 16(10): 1761-9.

[121] Barton KN, Stricker H, Elshaikh MA, *et al.*. Feasibility of Adenovirus-Mediated hNIS Gene Transfer and (131)I Radioiodine Therapy as a Definitive Treatment for Localized Prostate Cancer. Mol Ther 2011; 19(7): 1353-9.

[122] Penheiter AR, Griesmann GE, Federspiel MJ, Dingli D, Russell SJ, Carlson SK. Pinhole micro-SPECT/CT for noninvasive monitoring and quantitation of oncolytic virus dispersion and percent infection in solid tumors. Gene Ther 2011.

[123] Msaouel P, Dispenzieri A, Galanis E. Clinical testing of engineered oncolytic measles virus strains in the treatment of cancer: an overview. Curr Opin Mol Ther 2009; 11(1): 43-53.

[124] Li H, Peng KW, Dingli D, Kratzke RA, Russell SJ. Oncolytic measles viruses encoding interferon beta and the thyroidal sodium iodide symporter gene for mesothelioma virotherapy. Cancer Gene Ther 2010; 17(8): 550-8.

[125] Peerlinck I, Merron A, Baril P, *et al.*. Targeted radionuclide therapy using a Wnt-targeted replicating adenovirus encoding the Na/I symporter. Clin Cancer Res 2009; 15(21): 6595-601.

[126] Trujillo MA, Oneal MJ, Davydova J, Bergert E, Yamamoto M, Morris JC, 3rd. Construction of an MUC-1 promoter driven, conditionally replicating adenovirus that expresses the sodium iodide symporter for gene therapy of breast cancer. Breast Cancer Res 2009; 11(4): R53.

[127] Trujillo MA, Oneal MJ, McDonough S, Qin R, Morris JC. A probasin promoter, conditionally replicating adenovirus that expresses the sodium iodide symporter (NIS) for radiovirotherapy of prostate cancer. Gene Ther 2010; 17(11): 1325-32.

[128] Haddad D, Chen NG, Zhang Q, *et al.*. Insertion of the human sodium iodide symporter to facilitate deep tissue imaging does not alter oncolytic or replication capability of a novel vaccinia virus. J Transl Med 2011; 9: 36.

[129] Terrovitis J, Kwok KF, Lautamaki R, *et al.*. Ectopic expression of the sodium-iodide symporter enables imaging of transplanted cardiac stem cells *in vivo* by single-photon emission computed tomography or positron emission tomography. J Am Coll Cardiol 2008; 52(20): 1652-60.

[130] Welling MM, Duijvestein M, Signore A, van der Weerd L. *In vivo* biodistribution of stem cells using molecular nuclear medicine imaging. J Cell Physiol 2011; 226(6): 1444-52.

[131] Higuchi T, Anton M, Saraste A, *et al.*. Reporter gene PET for monitoring survival of transplanted endothelial progenitor cells in the rat heart after pretreatment with VEGF and atorvastatin. J Nucl Med 2009; 50(11): 1881-6.

[132] Seo JH, Jeon YH, Lee YJ, *et al.*. Trafficking macrophage migration using reporter gene imaging with human sodium iodide symporter in animal models of inflammation. J Nucl Med 2010; 51(10): 1637-43.

[133] Bloomfield PM, Rajeswaran S, Spinks TJ, *et al.*. The design and physical characteristic of a small animal positron emission tomograph. Phys Med Biol 1995; 40(6): 1105.

[134] Schafers KP, Reader AJ, Kriens M, Knoess C, Schober O, Schafers M. Performance evaluation of the 32-module quadHIDAC small-animal PET scanner. J Nucl Med 2005; 46(6): 996-1004.

[135] Del Guerra A, Belcari N. Advances in animal PET scanners. Q J Nucl Med 2002; 46(1): 35-47.

[136] Forrer F, Valkema R, Bernard B, *et al.*. *In vivo* radionuclide uptake quantification using a multi-pinhole SPECT system to predict renal function in small animals. Eur J Nucl Med Mol Imaging 2006; 33(10): 1214-7.

[137] Seo Y, Gao DW, Hasegawa BH, Dae MW, Franc BL. Rodent brain imaging with SPECT/CT. Med Phys 2007; 34(4): 1217-20.

[138] Beekman F, van der Have F. The pinhole: gateway to ultra-high-resolution three-dimensional radionuclide imaging. Eur J Nucl Med Mol Imaging 2007; 34(2): 151-61.

[139] Franc BL, Acton PD, Mari C, Hasegawa BH. Small-animal SPECT and SPECT/CT: important tools for preclinical investigation. J Nucl Med 2008; 49(10): 1651-63.

[140] van der Have F, Vastenhouw B, Ramakers RM, *et al.*. U-SPECT-II: An Ultra-High-Resolution Device for Molecular Small-Animal Imaging. J Nucl Med 2009; 50(4): 599-605.

[141] Magota K, Kubo N, Kuge Y, Nishijima K, Zhao S, Tamaki N. Performance characterization of the Inveon preclinical small-animal PET/SPECT/CT system for multimodality imaging. Eur J Nucl Med Mol Imaging 2011; 38(4): 742-52.

[142] Branderhorst W, Vastenhouw B, van der Have F, Blezer EL, Bleeker WK, Beekman FJ. Targeted multi-pinhole SPECT. Eur J Nucl Med Mol Imaging 2011; 38(3): 552-61.

[143] Cheng D, Wang Y, Liu X, *et al.*. Comparison of 18F PET and 99mTc SPECT imaging in phantoms and in tumored mice. Bioconjug Chem 2010; 21(8): 1565-70.

[144] King MA, Pretorius PH, Farncombe T, Beekman FJ. Introduction to the physics of molecular imaging with radioactive tracers in small animals. J Cell Biochem Suppl 2002; 39: 221-30.

[145] Ljunberg M, Sjogreen K, Liu X, Frey E, Dewaraja Y, Strand SE. A 3-dimensional absorbed dose calculation method based on quantitative SPECT for radionuclide therapy: evaluation for I-131 using Monte Carlo simulation. J Nucl Med 2002; 43: 1101-9.

[146] King M, Farncombe T. An overview of attenuation and scatter correction of planar and SPECT data for dosimetry studies. Cancer Biother Radiopharm 2003; 18(2): 181-90.

[147] Chatziloannou AF. Instrumentation for molecular imaging in preclinical research. Proc Am Thorac Soc 2005; 2: 533-6.

[148] Rowland DJ, Cherry SR. Small-animal preclinical nuclear medicine instrumentation and methodology. Semin Nucl Med 2008; 38(3): 209-22.

[149] Kagadis GC, Loudos G, Katsanos K, Langer SG, Nikiforidis GC. *In vivo* small animal imaging: current status and future prospects. Med Phys 2010; 37(12): 6421-42.

[150] Niu G, Krager KJ, Graham MM, Hichwa RD, Domann FE. Noninvasive radiological imaging of pulmonary gene transfer and expression using the human sodium iodide symporter. Eur J Nucl Med Mol Imaging 2005; 32(5): 534-40.

[151] Biersack HJ, Freeman LM. Clinical nuclear medicine. Berlin ; New York: Springer; 2007.

[152] Jauregui-Osoro M, Sunassee K, Weeks AJ, *et al.*. Synthesis and biological evaluation of [(18)F]tetrafluoroborate: a PET imaging agent for thyroid disease and reporter gene imaging of the sodium/iodide symporter. Eur J Nucl Med Mol Imaging. 2010; 37(11): 2108-16.

[153] Youn H, Jeong JM, Chung JK. A new PET probe, (18)F-tetrafluoroborate, for the sodium/iodide symporter: possible impacts on nuclear medicine. Eur J Nucl Med Mol Imaging 2010; 37(11): 2105-7.

[154] Vadysirisack DD, Shen DH, Jhiang SM. Correlation of Na+/I-symporter expression and activity: implications of Na+/I-symporter as an imaging reporter gene. J Nucl Med 2006; 47(1): 182-90.

[155] Gambhir SS, Bauer E, Black ME, *et al.*. A mutant herpes simplex virus type 1 thymidine kinase reporter gene shows improved sensitivity for imaging reporter gene expression with positron emission tomography. Proc Natl Acad Sci U S A 2000; 97(6): 2785-90.

[156] Gambhir SS, Herschman HR, Cherry SR, *et al.*. Imaging transgene expression with radionuclide imaging technologies. Neoplasia 2000; 2(1-2): 118-38.

[157] Luker GD, Luker KE. Optical imaging: current applications and future directions. J Nucl Med 2008; 49(1): 1-4.

[158] He Z, Evelhoch JL, Mohammad RM, Adsay NV, Pettit GR, Vaitkevicius VK, *et al.*. Magnetic resonance imaging to measure therapeutic response using an orthotopic model of human pancreatic cancer. Pancreas 2000; 21(1): 69-76.

[159] Wunderbaldinger P, Bogdanov A, Weissleder R. New approaches for imaging in gene therapy. Eur J Radiol 2000; 34(3): 156-65.

[160] Gilad AA, Ziv K, McMahon MT, van Zijl PC, Neeman M, Bulte JW. MRI reporter genes. J Nucl Med 2008; 49(12): 1905-8.

[161] Sharma V, Luker GD, Piwnica-Worms D. Molecular imaging of gene expression and protein function *in vivo* with PET and SPECT. J Magn Reson Imaging 2002; 16(4): 336-51.

[162] Neve KA, Cox BA, Henningsen RA, Spanoyannis A, Neve RL. Pivotal role for aspartate-80 in the regulation of dopamine D2 receptor affinity for drugs and inhibition of adenylyl cyclase. Mol Pharmacol 1991; 39(6): 733-9.

[163] Kang JH, Lee DS, Paeng JC, *et al.*. Development of a sodium/iodide symporter (NIS)-transgenic mouse for imaging of cardiomyocyte-specific reporter gene expression. J Nucl Med 2005; 46(3): 479-83.

[164] Kemerink GJ, Visser MG, Franssen R, *et al.*. Effect of the positron range of 18F, 68Ga and 124I on PET/CT in lung-equivalent materials. Eur J Nucl Med Mol Imaging 2011; 38(5): 940-8.

[165] Lubberink M, Herzog H. Quantitative imaging of 124I and 86Y with PET. Eur J Nucl Med Mol Imaging 2011; 38 Suppl 1: S10-8.

[166] Jentzen W, Freudenberg L, Bockisch A. Quantitative imaging of 124I with PET/ CT in pretherapy lesion dosimetry Effects impairing image quantification and their corrections. Q J Nucl Med Mol Imaging 2011; 55(1): 21-43.

[167] Liang Q, Satyamurthy N, Barrio JR, *et al.*. Noninvasive, quantitative imaging in living animals of a mutant dopamine D2 receptor reporter gene in which ligand binding is uncoupled from signal transduction. Gene Ther 2001; 8(19): 1490-8.

[168] MacLaren DC, Gambhir SS, Satyamurthy N, *et al.*. Repetitive, non-invasive imaging of the dopamine D2 receptor as a reporter gene in living animals. Gene Ther 1999; 6(5): 785-91.

[169] Ogawa O, Umegaki H, Ishiwata K, *et al.*. *In vivo* imaging of adenovirus-mediated over-expression of dopamine D2 receptors in rat striatum by positron emission tomography. Neuroreport 2000; 11(4): 743-8.

[170] Umegaki H, Ishiwata K, Ogawa O, *et al.*. *In vivo* assessment of adenoviral vector-mediated gene expression of dopamine D(2) receptors in the rat striatum by positron emission tomography. Synapse 2002; 43(3): 195-200.

[171] Herschman HR. Noninvasive imaging of reporter gene expression in living subjects. Adv Cancer Res 2004; 92: 29-80.

[172] Saito Y, Price RW, Rottenberg DA, *et al.*. Quantitative autoradiographic mapping of herpes simplex virus encephalitis

with a radiolabeled antiviral drug. Science 1982; 217(4565): 1151-3.

[173] Tjuvajev JG, Stockhammer G, Desai R, *et al.*. Imaging the expression of transfected genes *in vivo*. Cancer Res 1995; 55(24): 6126-32.

[174] Tjuvajev JG, Finn R, Watanabe K, *et al.*. Noninvasive imaging of herpes virus thymidine kinase gene transfer and expression: a potential method for monitoring clinical gene therapy. Cancer Res 1996; 56(18): 4087-95.

[175] Tjuvajev JG, Doubrovin M, Akhurst T, *et al.*. Comparison of radiolabeled nucleoside probes (FIAU, FHBG, and FHPG) for PET imaging of HSV1-tk gene expression. J Nucl Med 2002; 43(8): 1072-83.

[176] Min JJ, Iyer M, Gambhir SS. Comparison of [18F]FHBG and [14C]FIAU for imaging of HSV1-tk reporter gene expression: adenoviral infection vs stable transfection. Eur J Nucl Med Mol Imaging 2003; 30(11): 1547-60.

[177] Miyagawa T, Gogiberidze G, Serganova I, *et al.*. Imaging of HSV-tk Reporter gene expression: comparison between [18F]FEAU, [18F]FFEAU, and other imaging probes. J Nucl Med 2008; 49(4): 637-48.

[178] Ruggiero A, Brader P, Serganova I, *et al.*. Different strategies for reducing intestinal background radioactivity associated with imaging HSV1-tk expression using established radionucleoside probes. Mol Imaging 2010; 9(1): 47-58.

[179] Brust P, Haubner R, Friedrich A, *et al.*. Comparison of [18F]FHPG and [124/125I]FIAU for imaging herpes simplex virus type 1 thymidine kinase gene expression. Eur J Nucl Med 2001; 28(6): 721-9.

[180] Freytag SO, Barton KN, Brown SL, *et al.*. Replication-competent adenovirus-mediated suicide gene therapy with radiation in a preclinical model of pancreatic cancer. Mol Ther 2007; 15(9): 1600-6.

[181] Chaudhuri TR, Rogers BE, Buchsbaum DJ, Mountz JM, Zinn KR. A noninvasive reporter system to image adenoviral-mediated gene transfer to ovarian cancer xenografts. Gynecol Oncol 2001; 83(2): 432-8.

[182] Zinn KR, Chaudhuri TR, Krasnykh VN, *et al.*. Gamma camera dual imaging with a somatostatin receptor and thymidine kinase after gene transfer with a bicistronic adenovirus in mice. Radiology 2002; 223(2): 417-25.

[183] Zinn KR, Chaudhuri TR. The type 2 human somatostatin receptor as a platform for reporter gene imaging. Eur J Nucl Med Mol Imaging 2002; 29(3): 388-99.

[184] Rogers BE, Parry JJ, Andrews R, Cordopatis P, Nock BA, Maina T. MicroPET imaging of gene transfer with a somatostatin receptor-based reporter gene and (94m)Tc-Demotate 1. J Nucl Med 2005; 46(11): 1889-97.

[185] Schellingerhout D. Molecular imaging of novel cell- and viral-based therapies. Neuroimaging Clin N Am 2006; 16(4): 655-79, ix.

[186] Cotugno G, Aurilio M, Annunziata P, *et al.*. Noninvasive repetitive imaging of somatostatin receptor 2 gene transfer with positron emission tomography. Hum Gene Ther 2011; 22(2):189-96.

[187] Moroz MA, Serganova I, Zanzonico P, *et al.*. Imaging hNET reporter gene expression with 124I-MIBG. J Nucl Med 2007; 48(5): 827-36.

[188] Brader P, Kelly KJ, Chen N, *et al.*. Imaging a Genetically Engineered Oncolytic Vaccinia Virus (GLV-1h99) Using a Human Norepinephrine Transporter Reporter Gene. Clin Cancer Res 2009; 15(11): 3791-801.

[189] Altmann A, Kissel M, Zitzmann S, *et al.*. Increased MIBG uptake after transfer of the human norepinephrine transporter gene in rat hepatoma. J Nucl Med 2003; 44(6): 973-80.

[190] Anton M, Wagner B, Haubner R, *et al.*. Use of the norepinephrine transporter as a reporter gene for non-invasive imaging of genetically modified cells. J Gene Med 2004; 6(1): 119-26.

[191] Weeks AJ, Jauregui-Osoro M, Cleij M, Blower JE, Ballinger JR, Blower PJ. Evaluation of [18F]-tetrafluoroborate as a potential PET imaging agent for the human sodium/iodide symporter in a new colon carcinoma cell line, HCT116, expressing hNIS. Nucl Med Commun 2011; 32(2): 98-105.

Received: August 17, 2011 **Revised: January 04, 2012** **Accepted: January 06, 2012**